Vol. 687: 147–162, 2022
https://doi.org/10.3354/meps14010

MARINE ECOLOGY PROGRESS SERIES
Mar Ecol Prog Ser

Published April 7

Impaired hatching exacerbates the high CO_2 sensitivity of embryonic sand lance *Ammodytes dubius*

Hannes Baumann[1,*], Lucas F. Jones[1], Christopher S. Murray[2], Samantha A. Siedlecki[1], Michael Alexander[3], Emma L. Cross[4]

[1]University of Connecticut, Department of Marine Sciences, 1080 Shennecossett Road, Groton, CT 06340, USA

[2]School of Marine and Environmental Affairs and Washington Ocean Acidification Center, University of Washington, 3710 Brooklyn Ave NE, Seattle, WA 98105, USA

[3]NOAA Physical Sciences Laboratory, Boulder, CO 80305-3328, USA

[4]Southern Connecticut State University, Department of the Environment, Geography, and Marine Sciences, 501 Crescent Street, New Haven, CT 06515, USA

ABSTRACT: Rising oceanic partial pressure of CO_2 (pCO_2) could affect many traits in fish early life stages, but only few species to date have shown direct CO_2-induced survival reductions. This might partly be because species from less CO_2-variable, offshore environments in higher latitudes are currently underrepresented in the literature. We conducted new experimental work on northern sand lance *Ammodytes dubius*, a key forage fish on offshore Northwest Atlantic sand banks, which was recently suggested to be highly CO_2-sensitive. In 2 complementary trials, we produced embryos from wild, Gulf of Maine spawners and reared them at several pCO_2 levels (~400–2000 µatm) in combination with static (6, 7, 10°C) and dynamic (10→5°C) temperature treatments. Again, we consistently observed large, CO_2-induced reductions in hatching success (−23% at 1000 µatm, −61% at ~2000 µatm), and the effects were temperature-independent. To distinguish pCO_2 effects during development from potential impacts on hatching itself, some embryos were switched between high and control pCO_2 treatments just prior to hatch. This indeed altered hatching patterns, consistent with the CO_2-impaired hatching hypothesis. High CO_2 also delayed the day of first hatch in one trial and peak hatch in the other, where later-hatched larvae were of similar size but with progressively less endogenous energy reserves. For context, we extracted seasonal pCO_2 projections for Stellwagen Bank (Gulf of Maine) from regional ensemble simulations, which indicated a CO_2-induced reduction in sand lance hatching success to 71% of contemporary levels by 2100. The species' unusual CO_2 sensitivity has large ecological and scientific ramifications that warrant future in-depth research.

KEY WORDS: Ocean acidification · CO_2-impaired hatching · Dynamic temperature · Endogenous energy reserves · Regional pCO_2 projections

1. INTRODUCTION

Anthropogenic ocean warming and acidification continue to accelerate globally (Garcia-Soto et al. 2021) and thus lend urgency to the question of how marine organisms will cope with novel emerging climates (Lotterhos et al. 2021). Over recent decades, CO_2 exposure experiments have provided first answers by aiming to distinguish CO_2-sensitive from CO_2-tolerant organisms and traits and by elucidating mechanisms and stressor interactions (Boyd et al. 2018, Baumann 2019). This revealed that many traits in a majority of taxa are potentially sensitive to changing CO_2 conditions (Harvey et al. 2013, Cat-

*Corresponding author: hannes.baumann@uconn.edu

Publisher: Inter-Research · www.int-res.com

tano et al. 2018, Doney et al. 2020). It implies fundamental shifts to the fitness landscape in future high-CO_2 oceans (Munday et al. 2019), but specific predictions are still beset by unresolved questions of adaptation (Sunday et al. 2014) and the notorious heterogeneity of experimental trait responses to high CO_2 across all levels of taxonomic organization (Kroeker et al. 2013, Busch et al. 2015, Przeslawski et al. 2015).

Experiments on marine fish have shown that short-term high CO_2 exposures can reduce survival in some but not most tested species and that such lethal effects occur almost exclusively at the earliest, least developed life stages (Baumann et al. 2012, Dahlke et al. 2020). Other responses to acidified conditions comprise non-lethal changes to e.g. gene expression (e.g. Porteus et al. 2018, Mazurais et al. 2020), metabolism (e.g. Munday et al. 2009, Pimentel et al. 2014, Crespel et al. 2019), growth and morphometry (e.g. Bignami et al. 2013, Perry et al. 2015, Murray & Baumann 2020), behavior (Ashur et al. 2017) or reproduction (e.g. Faria et al. 2018, Concannon et al. 2021), which are by-products of most fishes' capacity for swift CO_2 acclimation and effective acid–base regulation (Esbaugh 2018). Non-lethal CO_2 effects may still inflict real fitness costs (e.g. aberrant behavior could increase predation mortality; Munday et al. 2012), but this is more often assumed than explicitly shown.

Interestingly, one of the more consistent experimental findings has been that parental CO_2 environments modulate offspring CO_2 sensitivities in most studied taxa (Murray et al. 2014, Donelson et al. 2018). Since aquatic habitats differ vastly in their degree of diel, seasonal, or ephemeral CO_2 fluctuations even across small spatial scales (Hofmann et al. 2011), the complex mosaic of species' CO_2 sensitivities might therefore not be surprising. Indeed, recent analyses concluded exactly this for select echinoderm, mollusk, and copepod species, showing that the more CO_2-tolerant groups were those sourced from more CO_2-extreme and CO_2-variable environments (Kelly et al. 2013, Vargas et al. 2017). The ocean variability hypothesis (Baumann 2019) arguably applies to fishes as well, but current data likely over-represent CO_2-tolerant species from more accessible nearshore, metabolically active environments (Franke & Clemmesen 2011, Depasquale et al. 2015, Lonthair et al. 2017). There, contemporary CO_2 fluctuations already exceed average surface ocean projections decades and centuries from now (Baumann et al. 2015, Doney et al. 2020). In contrast, the fewer cases of direct CO_2 sensitivity (i.e. reduced survival) appear to occur in fishes that are adapted to less CO_2-variable, offshore habitats closer to atmospheric equilibrium (i.e. ~400 µatm; e.g. Chambers et al. 2014, Stiasny et al. 2016, Dahlke et al. 2017, Alter & Peck 2021).

High early life CO_2 sensitivity in fishes could also depend on slow rates of early life development, as seen in most cold-water species from temperate to polar environments (Baumann 2019). This may allow CO_2 effects to accumulate while embryos are still maturing the cellular structures for acid–base regulation and thus lead to acidosis, which is so far the presumed mechanism causing all CO_2-induced survival effects in fish early life stages (Heuer & Grosell 2014). In contrast, most tropical and subtropical fishes develop into acid–base competent, active swimmers mere days after fertilization and therefore likely before detectable lethal CO_2 effects can accrue (Pimentel et al. 2014, Munday et al. 2016). Albeit intuitive, these emergent patterns still require further empirical corroboration, particularly from candidate species chosen more strategically, i.e. from more offshore habitats at temperate to polar latitudes. Such fishes could prove more CO_2-sensitive and thus more vulnerable to climate change than currently appreciated.

Consider thus the slender-bodied sand lances (Ammodytidae), which are key forage fishes in temperate to polar ecosystems in the northern hemisphere (Staudinger et al. 2020). In some areas, their high local abundance and nutritious quality alone appear to sustain local diversity hotspots of higher trophic piscivores, as for example on Stellwagen Bank in the southern Gulf of Maine (Fig. S1 in the Supplement at www.int-res.com/articles/suppl/m687p147_supp.pdf; see also Suca et al. 2021). Here, dense aggregations of northern sand lance (*Ammodytes dubius*, hereafter sand lance) attract predators such as cod, tuna, and sharks, in addition to foraging seabirds, seals, dolphins, and humpback whales (Silva et al. 2020, Staudinger et al. 2020). Sand lances are gonochoristic, iteroparous fish that mature at 1–2 yr of age and can live up to 8 yr, although most in the Gulf of Maine are ≤5 yr old (Staudinger et al. 2020). Importantly, sand lance are winter spawners, which causes their demersal embryos to develop very slowly over weeks and larvae to emerge in time to utilize the first productivity bloom of the new year (Robards et al. 2000). Larvae can remain pelagic for 2–3 mo, before settling as juveniles on offshore, coarse-grain sand banks across the Northwest Atlantic shelf (Suca et al. 2021).

For these reasons, we recently began studying the CO_2 sensitivity of sand lance offspring in factorial rearing experiments, with striking results (Murray et al. 2019). Embryos showed some of the strongest CO_2-induced survival reductions documented yet among fishes (up to −90% at ~2000 versus 400 µatm CO_2). Intriguingly, we noticed that many embryos at high CO_2 treatments did not merely arrest their development (indicative of acidosis), but appeared fully developed and 'ready' to hatch but incapable of doing so. We therefore hypothesize that, in addition to acidosis, high CO_2 directly impairs hatching in sand lance, potentially via affecting the production or efficacy of choreolytic hatching enzymes, but this requires additional data and more targeted tests. Moreover, the species' apparent CO_2 sensitivity alone demands further empirical evaluations ('you better repeat it'; Murray & Baumann 2018) as well as context to specific partial pressure of CO_2 (pCO_2) projections for its natural habitat. We thus conducted further CO_2 × temperature experiments on sand lance from the same population in the southern Gulf of Maine (Stellwagen Bank National Marine Sanctuary, SBNMS). Beyond replication, we aimed to identify potential CO_2-sensitivity thresholds by testing additional CO_2 levels and employed 2 complementary approaches to explore the CO_2-impaired hatching hypothesis. Finally, we compared our experimental findings to recent, seasonally explicit pCO_2 projections for Stellwagen Bank in 2050 and 2100 based on Siedlecki et al. (2021) to begin constraining the species' potential climate vulnerability.

2. MATERIALS AND METHODS

2.1. Experimental setup

Two complementary experiments were conducted in late 2018 (Expt 1) and 2020 (Expt 2), each rearing newly fertilized sand lance embryos to hatch over the course of 32–65 d. Founder adults were sampled at SBNMS (42° 9′ 58.26″ N, 70° 18′ 44.19″ W) at the peak of their narrow, local spawning window on 15 (Expt 1) or 27 November (Expt 2), using a 1.3 × 0.7 m beam trawl (6 mm mesh) towed over ground at 3 knots for 15 min. On deck, all flowing-ripe males and females were strip-spawned together (at 10°C, Expt 1: $N_{male/female}$ = 29/13; Expt 2: $N_{male/female}$ = 50/46) and their progeny were transported to the University of Connecticut's Rankin Seawater Lab. There, exposure experiments commenced within 8 h post-fertilization by placing a volumetrically measured random sample of 600 (Expt 1) or 1200 embryos (Expt 2) into each replicate rearing container.

Rearing containers (750 ml plastic cups) were fitted with 100 µm mesh bottoms and received a gravity-fed flow of approximately 4 l h^{-1}, while floating in larger recirculating treatment tanks (600 l) controlled for temperature, pH, and oxygen conditions (Automated Larval Fish Rearing System, ALFiRiS). Briefly, ALFiRiS works by pumping treatment water past a central pH electrode (Hach pHD, cross-checked daily with an independent Hach Intellical PHC281 sensor on a HQ11D handheld pH/ORP meter, both being calibrated weekly with 2-point National Institute of Standards and Technology [NIST] pH standards) and an optical dissolved oxygen sensor (Hach LDO Model 2) to sequentially monitor experimental conditions in each of 9 independent units. Customized LabView (National Instruments) routines then control solenoid valves connected to pressurized CO_2 (bone-dry grade), N_2, and CO_2-stripped air (for details, see Murray et al. 2019). Between Expts 1 and 2, ALFiRiS' temperature system was upgraded from manually set thermostats (Expt 1) to LabView control (Expt 2) over relay loops that activate heaters/chillers, to now allow dynamic, computer-controlled temperature treatments. Experimental seawater was drawn from subsurface eastern Long Island Sound (31 psu), filtered to 1 µm, and UV-sterilized before use. Oxygen levels were maintained at ~100% saturation, while the photoperiod was 11 h light:13 h dark. Ten percent of seawater in each unit was replaced weekly.

2.2. Seawater chemistry

Realized pCO_2 conditions and other seawater chemistry parameters (Table 1) were estimated in CO2SYS (V2.1, Pierrot et al. 2006) based on samples taken every 10 d and measured for temperature, pH_{NIST}, salinity (refractometer, Cole-Parmer, ±0.3%) and total alkalinity (A_T, µmol kg^{-1}). Seawater samples were filtered to 10 µm, stored in 300 ml borosilicate bottles at 3°C, and within days measured for A_T using endpoint titration (Mettler Toledo G20 Potentiometric Titrator) with an accuracy of ±1% (Murray et al. 2019; verified and calibrated using Dr. Andrew Dickson's certified reference material for A_T in seawater; Scripps Institution of Oceanography, batch nos. 162 and 164).

2.3. Experimental design

During Expt 1, we tested factorial combinations of 2 static temperatures and 3 target pCO_2 levels,

Table 1. Experimental conditions and seawater chemistry during Expts 1 (2018) and 2 (2020). Mean (±SD) pH_{NIST} and temperature from hourly records, total alkalinity (A_T) from replicated seawater water samples, partial pressure and fugacity of CO_2 (pCO_2 and fCO_2), dissolved inorganic carbon (C_T), and carbonate ion concentration (CO_3^{2-}) calculated with CO2SYS (V2.1)

	Temperature (°C)	pH	A_T (µmol kg^{-1})	pCO_2 (µatm)	C_T (µmol kg^{-1})	fCO_2 (µatm)	CO_3^{2-} (µmol kg^{-1})
Expt 1, 2018	5.8 ± 0.5	8.12 ± 0.02	2022 ± 13	391 ± 9	1914 ± 12	390 ± 9	84 ± 2
	5.9 ± 0.2	7.75 ± 0.06	2019 ± 13	946 ± 68	2009 ± 20	942 ± 67	39 ± 2
	5.9 ± 0.8	7.47 ± 0.06	2025 ± 6	1828 ± 89	2089 ± 10	1820 ± 88	21 ± 1
Expt 2, 2020	7.1 ± 0.8	8.10 ± 0.04	2152 ± 31	436 ± 35	2034 ± 31	434 ± 35	93 ± 8
	7.1 ± 0.8	7.76 ± 0.05	2152 ± 39	993 ± 44	2132 ± 41	989 ± 43	46 ± 1
	7.1 ± 1.0	7.64 ± 0.02	2139 ± 36	1344 ± 43	2154 ± 38	1338 ± 42	34 ± 1
	7.3 ± 1.0	7.54 ± 0.05	2149 ± 30	1674 ± 50	2189 ± 32	1667 ± 49	28 ± 1
	7.2 ± 1.0	7.47 ± 0.04	2142 ± 28	1995 ± 70	2205 ± 32	1987 ± 70	24 ± 0
Expt 1, 2018	10.0 ± 0.4	8.12 ± 0.02	2031 ± 32	437 ± 40	1908 ± 38	435 ± 40	94 ± 6
	10.2 ± 0.3	8.04 ± 0.02	2025 ± 3	530 ± 49	1927 ± 12	528 ± 48	80 ± 6
	10.4 ± 0.4	7.95 ± 0.03	2022 ± 9	663 ± 33	1951 ± 7	661 ± 33	66 ± 3
	10.1 ± 0.3	7.85 ± 0.03	2032 ± 19	839 ± 58	1987 ± 15	835 ± 57	54 ± 4
	10.1 ± 0.4	7.76 ± 0.03	2028 ± 16	1010 ± 17	2003 ± 15	1007 ± 17	46 ± 1
	10.2 ± 0.4	7.46 ± 0.07	2021 ± 8	1992 ± 47	2073 ± 5	1985 ± 47	25 ± 1
Expt 2, 2020	10 → 5	8.11 ± 0.04	2154 ± 24	416 ± 40	2037 ± 18	414 ± 36	92 ± 8
	10 → 5	7.77 ± 0.03	2152 ± 22	976 ± 50	2136 ± 23	972 ± 48	44 ± 1
	10 → 5	7.63 ± 0.04	2159 ± 32	1336 ± 72	2179 ± 32	1331 ± 72	33 ± 2
	10 → 5	7.48 ± 0.05	2149 ± 28	1928 ± 138	2213 ± 28	1921 ± 137	23 ± 1

thereby encompassing contemporary thermal conditions on Stellwagen Bank between late fall (10°C) and early winter (6°C), as well as current ambient (400 µatm, pH~8.12), predicted end-of-century (1000 µatm, pH~7.76), and maximum open ocean pCO_2 benchmarks (2000 µatm, pH~7.48; Caldeira & Wickett 2003, Salisbury & Jönsson 2018). At 10°C, 3 additional pCO_2 levels below 1000 µatm (570, 690, 890 µatm; Table 1) were included to better describe near-future CO_2 sensitivities of sand lance embryos. The replication level for each of the 9 treatments was N = 5. Prior to hatch, 50 embryos per replicate were subsampled (150–200 degree-days post-fertilization, ddpf) and preserved in RNAlater for future analyses (to be reported elsewhere). Another 50 embryos per replicate were subsampled at 90–190 ddpf and preserved in buffered (sodium tetraborate) 5% formaldehyde/freshwater solution. Embryos sampled just before hatching began (170 ddpf, one random replicate per treatment) were later submitted for sectioning and staining (H&E stain; Horus Scientific) and then imaged for analyses of chorionic thickness (Nikon SMZ-1000 with Luminera Infinity2-2 camera and ImagePro Premier V9.0, Media Cybernetics).

During Expt 2, we again targeted pCO_2 levels of 400, 1000, and 2000 µatm, first at an intermediate static temperature of 7°C and second at a dynamic temperature of 10°C decreasing to 5°C at a rate of 0.2°C d^{-1} (10→5°C). The latter was chosen to approximate the seasonal decline in bottom temperatures experienced by sand lance embryos on Stellwagen Bank (Murray et al. 2019, Suca et al. 2021). The 2 treatments reached thermal equivalence at 32 dpf (224 ddfp) – just after hatching had started. To better describe sand lance upper CO_2 sensitivities (1000–2000 µatm), we added 2 intermediate pCO_2 levels at 7°C (~1300 and ~1700 µatm) and 1 at 10→5°C (~1300 µatm). The initial replication level for each of the 9 treatments was N = 6. However, to disentangle potential pCO_2 effects on embryonic development versus effects on hatching itself, we switched 3 random replicates from each extreme pCO_2 treatment per temperature with the opposite pCO_2 treatment (i.e. 3 × ~400→~2000 µatm and 3 × ~2000→~400 µatm). The switch happened at 175 ddpf (i.e. 25 dpf at 7°C; 22 dpf at 10→5°C), just before hatching started.

2.4. Response traits

From 90 ddpf onwards, rearing containers were monitored daily until hatching commenced; then, the number of hatchlings per replicate was recorded daily until hatching ceased. All hatchlings were immediately preserved in buffered 5% formaldehyde/freshwater solution for later morphological measurements. At the conclusion of Expt 1, unhatched remains were imaged at 4× magnification, allowing the later distinction between (a) early arrested embryos (no or only amorphous cell masses visible), (b) partially developed embryos (unpigmented eyes visible, body not fully wrapped around the egg), and (c) fully developed embryos (pigmented eyes, body clearly visible and more than 1× wrapped around; Fig. S2). In Expt 2, we continued daily monitoring for 7 more days after hatching had ceased, then examined the remains microscopically for embryos still alive (i.e. with beating hearts). Absolute hatching numbers were transformed to daily relative frequencies by dividing by the initial number of embryos that was adjusted for subsampling (Expt 1, N = 500 per replicate) or reduced fertilization success (Expt 2, N = 873 per replicate, based on examining independent post-fertilization subsamples). Relative frequencies were then summed to yield cumulative hatching success (HS, %) for each replicate. For Expt 1, we additionally calculated the proportions of (a) fully developed but unhatched embryos and (b) all other arrested embryos combined. The latter also included decayed stages that were no longer detectable at the conclusion of Expt 1.

To characterize hatching phenology, we recorded the day of first hatch (dpf), day of peak hatch (=dpf with the highest relative hatch frequency), and the total hatching period (d) for each replicate. Following Murray et al. (2019), a large number of hatchlings were imaged at 4× magnification (Expt 1: N_{total} = 3923; Expt 2: N_{total} = 2659) and then individually measured (ImagePro) for 3 morphological traits, i.e. standard length (SL, to the nearest 0.01 mm), yolk sac area (to the nearest 0.001 mm^2), and the size of the remaining oil globule inside the yolk sac (to the nearest 0.001 mm^2). The latter 2 traits are proxies for endogenous energy reserves (EER) after hatching, but they were strongly correlated ($N = 5552$, $R = 0.62$, $p < 0.001$). Hence, we used principal component analysis to extract PC1 (explaining 73% [Expt 1] and 81% [Expt 2] of variability) and then used the PC1 scores as the new variable, hereafter referred to as EER. Histological sections of fully developed, pre-hatch embryos from Expt 1 were imaged at 20× magnification to measure the thickness of the egg envelope (chorion, ImagePro). Chorion thickness was measured at 10 randomly selected locations around the circumference of the sectioned embryo, with measurements averaged subsequently for each embryo. Unfortunately, fewer than expected embryos were sectioned well enough for quality measurements, ranging from 2 to 7 per treatment.

All husbandry and experimental protocols were approved by the Institutional Animal Care and Use Committee (IACUC) of the University of Connecticut (nos. A17-043, A20-046).

2.5. Statistical analysis

For each experiment (Expts 1 and 2), we first used a general linear model (GLM) with temperature as a categorical fixed factor and pCO_2 as a continuous fixed factor to test for pCO_2, temperature, and pCO_2 × temperature effects on logit-transformed HS {$HS_{logit} = \log_{10}[HS/(1-HS)]$}, hatching phenology (day of first, peak hatch, hatch period), mean chorionic thickness (Expt 1 only), as well as hatch SL and EER of the initial hatch peaks (first 4 d of hatching). For traits showing significant pCO_2 effects ($p < 0.05$), we then used linear regression to further explore their relationships to pCO_2, first separately by experiment and temperature and then across all data based on replicate means.

For HS, we further calculated effect sizes as log-transformed response ratios (R_{HS}):

$$R_{HS\ (i,j,k,l)} = \ln(HS_{i,j,k,l}) - \ln(\overline{HS_{cont\ |\ k,l}}) \quad (1)$$

for each replicate i at pCO_2 level j, temperature k, and experiment l, based on the temperature- and experiment-specific mean HS at control pCO_2 (HS_{cont}, ~400 µatm). We then averaged R_{HS} and calculated bootstrapped 95% confidence intervals (95% CI) for each pCO_2 level, temperature, and experiment, and regressed these values linearly against pCO_2. This effectively standardized pCO_2 effects across temperatures and experiments with different HS baselines — an approach common in meta-analyses (Kroeker et al. 2010, Baumann et al. 2018, Cattano et al. 2018). Effects with 95% CIs excluding zero were considered significant. For Expt 2, we used a GLM for each temperature to test the null hypothesis that hatching success (HS_{logit}) did not differ between static (control or high) and switched pCO_2 groups (control→high; high→control, with group as a fixed factor, LSD post hoc tests). Rejection of the null hypothesis would suggest that pCO_2 influenced hatching itself, apart from effects on embryonic development. In addition, we used linear regression to test whether hatch SL and EER changed over the course of the extended hatching period during Expt 2. One treatment (Expt 2, 7°C, 1700 µatm pCO_2) showed consistent outlier values across several traits and all replicates (i.e. abnormally low HS, hatch SL, EER) and thus had to be excluded. Statistical analyses were computed using SPSS (V20 IBM).

2.6. Stellwagen Bank seasonal pCO_2 projections

To contextualize sand lance CO_2 sensitivities under future pCO_2 conditions, we utilized recent, high-resolution projections for the Gulf of Maine for the years 2050 and 2100 under the RCP 8.5 climate change scenario (Alexander et al. 2020). Three global projections (HadGEM2-ES: Hadley Center Earth System; GFDL: Geophysical Fluid Dynamics Lab; IPSL: Institut Pierre Simon Laplace) were downscaled using the Regional Ocean Modeling System (ROMS) with a 7 km horizontal resolution and 40 terrain-following vertical levels. The simulations were performed using the 'delta method', which provided estimates of future conditions for the average of a 30-yr period (2070–2100) centered on 2085. To obtain values for the year 2050, Brickman et al. (2021) uniformly scaled the temperature and salinity values by 0.546, based on the difference in the radiative forcing between 2085 and 2050. Similarly, we scaled the temperature (T) and salinity (S) values by 1.183 to represent the 2100 climate. Using an empirical model for dissolved inorganic carbon (DIC) and A_T (McGarry et al. 2021), the projected hydrography (T, S) was subsequently used to calculate DIC and A_T. Then, a slug of additional anthropogenic DIC was added assuming equilibrium with the projected atmospheric carbon dioxide in the future according to the emissions pathway, with further details described in Siedlecki et al. (2021). This approach has been shown to reproduce the seasonal cycle of aragonite saturation state (Ω) at the surface in the Gulf of Maine (Siedlecki et al. 2021). Monthly temperature, salinity, DIC, and A_T values in 2050 and 2100 were extracted from the simulations for the upper 40 m on Stellwagen Bank (bounded by 42.13°–42.5° N, 70.5°–70.12° W). DIC and A_T values were then used to calculate pCO_2 (µatm) using CO2SYS (V2.1). Values were also averaged for the 3 winter months (December to February), when sand lance embryos actually occur on the bank.

3. RESULTS

Mean HS under control pCO_2 conditions ranged from 49 to 58% in Expt 1 and 35 to 40% in Expt 2 (Fig. 1A). In both experiments, GLMs showed strong negative pCO_2 effects on HS regardless of thermal conditions (pCO_2: $p < 0.001$; temperature: $p > 0.3$; Table 2). Indeed, the 6°C and 10°C treatments during Expt 1, as well as the 7°C static and the 10→5°C dynamic treatments during Expt 2, showed consistent HS declines with pCO_2 (Fig. 1A). No temperature × pCO_2 interaction occurred. Thus, the linear regression model across all HS replicate means (R^2 = 0.59, $p < 0.001$) suggested an overall CO_2-induced HS decline from 47 ± 7% (95%CI) at control pCO_2 levels (400 µatm) to 36 ± 5% at 1000 µatm and 18 ±

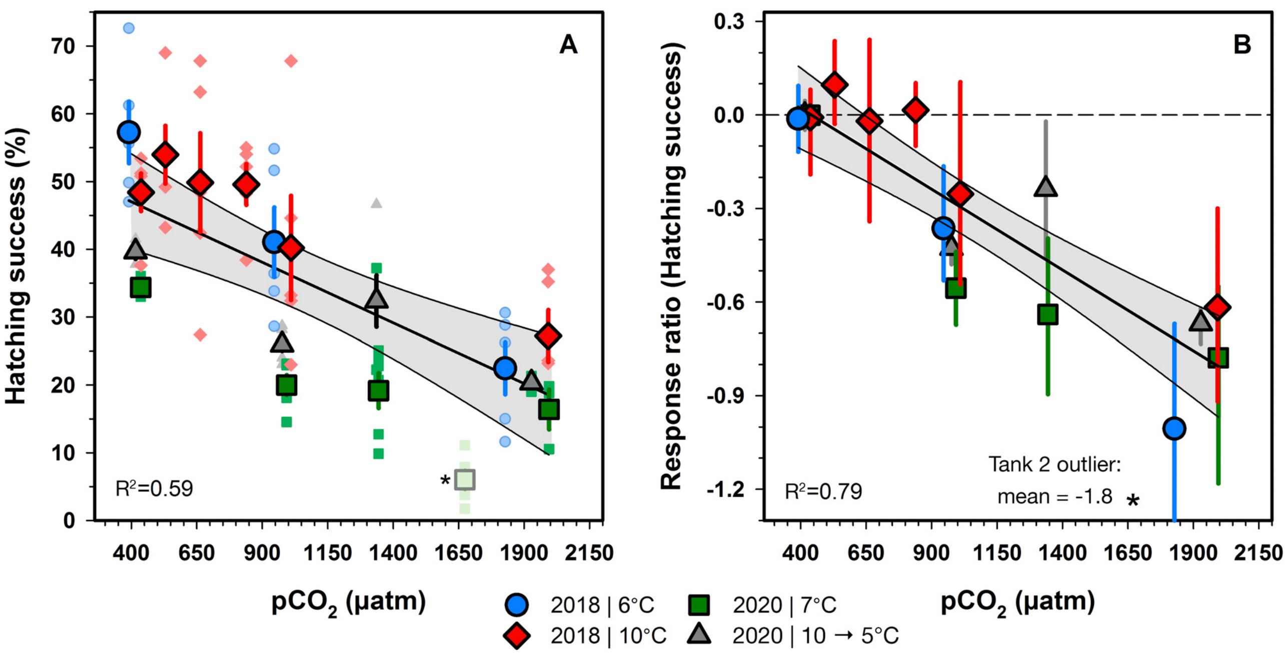

Fig. 1. CO_2 sensitivity of *Ammodytes dubius* hatching success (HS) during Expt 1 (6°C: blue circles; 10°C: red diamonds) and Expt 2 (7°C: green squares; 10→5°C: grey triangles): (A) Relative CO_2-specific HS, with small and large symbols depicting individual replicates and treatment means (±1 SE), respectively. (B) Mean CO_2-specific response ratios of HS (R_{HS} ± 95% CI). Black lines/shading: linear regressions ±95% confidence intervals based on replicate means. Asterisk: outlier tank 2 (Expt 2: 1700 µatm pCO_2), not included in regressions

Table 2. General linear model (GLM) p-values by experiment, testing for effects of temperature (fixed factor), CO_2 (continuous fixed factor), and their interaction on hatching success (logit-transformed), hatch length, endogenous reserves (=PC1, yolk sac, oil globule size), day of first and peak hatch, hatch period, and chorionic thickness (Expt 1). Significant effects ($p < 0.05$) are in **bold** (*p = 0.004, if the CO_2 × Temperature term is omitted from the GLM)

Response trait	Expt 1 I 2018			Expt 2 I 2020		
	CO_2	Temperature	CO_2 × Temperature	CO_2	Temperature	CO_2 × Temperature
Hatching success	**<0.001**	0.33	0.20	**<0.001**	0.42	0.54
Hatch length	**0.021**	**0.001**	0.12	0.88	0.43*	0.72
Endogenous reserves	0.41	0.06	0.65	0.94	0.06	0.80
First hatch	**0.001**	**<0.001**	0.65	Not computed, uniform		
Peak hatch	0.13	**<0.001**	0.99	**<0.001**	0.26	0.19
Hatch period	0.39	**0.001**	0.95	0.97	0.5	0.97
Chorionic thickness	**0.035**	0.54	0.33	Not assessed		

9 % at 2000 µatm, which are reductions of −23 % and −61 %, respectively (Fig. 1A). Controlling for different baseline levels of HS via response ratios (R_{HS}) strengthened the linear relationship ($R^2 = 0.79$, $p < 0.001$) and suggested that the negative effect on mean R_{HS} grew with each 500 µatm pCO_2 increase by −0.25 (Fig. 1B).

While HS declined with pCO_2, the proportion of fully developed but unhatched embryos at the conclusion of Expt 1 increased from 2–3 % at control pCO_2 to 19–22 % at ~2000 µatm pCO_2 (linear regression, $R^2 = 0.99$). Similarly, the proportion of arrested or decayed embryos increased from 40–49 % at pCO_2 controls to 53–58 % at ~2000 µatm pCO_2 ($R^2 = 0.69$; Fig. 2). During Expt 2, a negligible, pCO_2-independent proportion of unhatched embryos (0–0.6 %) remained alive 7 d after hatching had ceased. The switch of ready-to-hatch embryos from high to control pCO_2 increased HS compared to static high pCO_2 treatments at 7°C (E2; GLM, p = 0.09) and 10→5°C (GLM, p = 0.002; Fig. 3A,B). Conversely, the switch from control to high pCO_2 reduced HS in the 7°C treatment (GLM, p = 0.014, Fig. 3C), but had no effect in the 10→5°C treatment (GLM, p = 0.88; Fig. 3D).

During Expt 1, the 6°C hatchlings were significantly larger (mean $SL_{6°C}$ = 5.23 mm) than those at 10°C (mean $SL_{10°C}$ = 5.02 mm, GLM, p = 0.001; Fig. 4A). A weak positive pCO_2 effect (GLM, p = 0.021) was driven mostly by small SL values in just one treatment (10°C, control pCO_2), and there was no CO_2 × temperature interaction (GLM, p = 0.12). During Expt 2, pCO_2 did not affect hatch SL (p = 0.88; Table 2, Fig. 4A), and there were also no temperature or interactive effects. However, if the interaction term was omitted from the GLM, the temperature term became significant (p = 0.004), because embryos experiencing dynamic 10→5°C temperatures

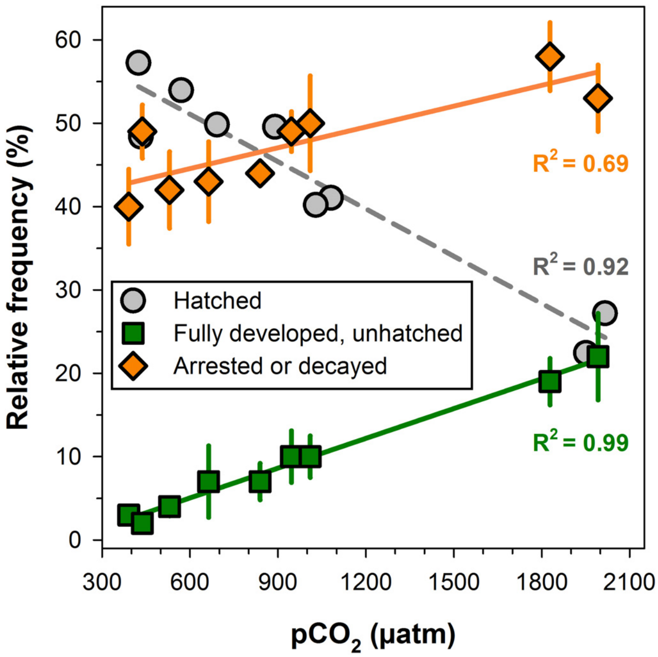

Fig. 2. Relative frequencies of hatched *Ammodytes dubius* larvae (grey circles, same as in Fig. 1A), fully developed but unhatched embryos (green squares), and arrested/decayed embryos (includes early arrests, partially developed, and decayed embryos; orange diamonds) at the conclusion of Expt 1. Symbols represent treatment means (±1 SE) across both temperatures, fitted with linear regressions (lines)

hatched with a greater mean (±SD) SL than their conspecifics in static 7°C treatments (first 4 d: 5.20 ± 0.16 mm versus 5.02 ± 0.19 mm, Fig. 4A; entire hatching period: 5.31 ± 0.09 mm versus 5.06 ± 0.22 mm, Fig. S3). Within Expts 1 and 2, EER varied independently of pCO_2 (p > 0.4) and temperature (p > 0.06, no interaction), but differed across experiments, because Expt 1 hatchlings had greater EER than those during Expt 2 (Fig.4B). Overall, we found EER to be

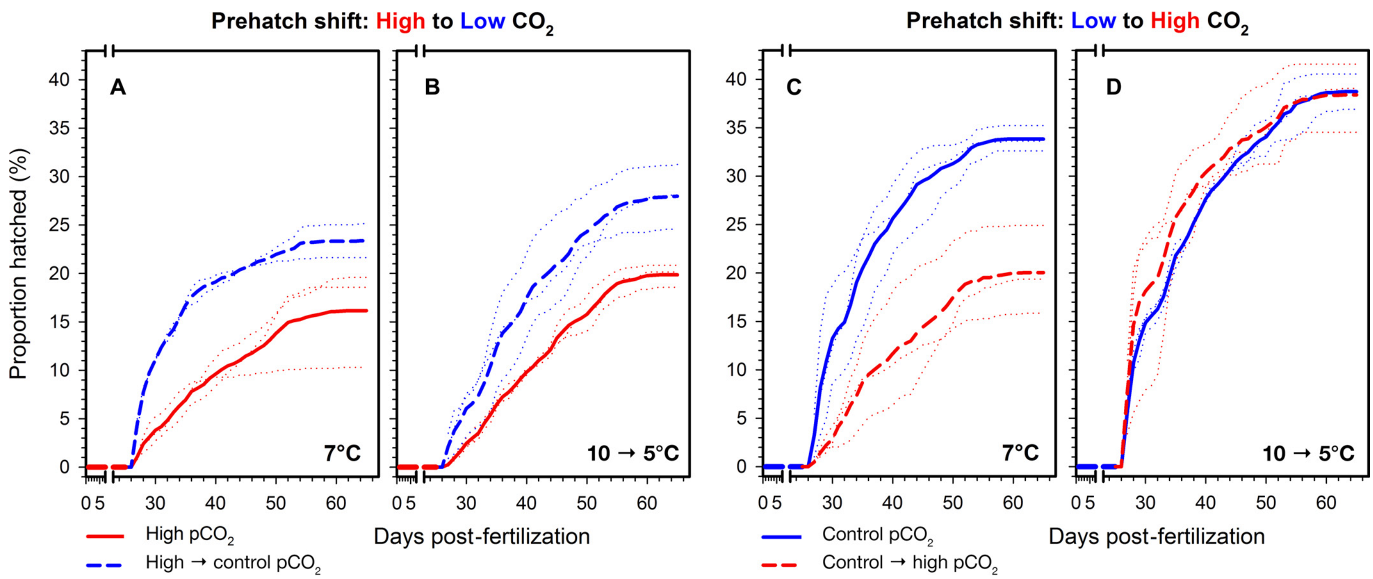

Fig. 3. Cumulative *Ammodytes dubius* hatching success in Expt 2 at 2 temperatures and either constant (solid lines) or shifted CO_2 conditions (dashed lines). (A,B) Embryos developing at high CO_2 conditions (~2000 µatm), with one half of the replicates shifted pre-hatch to control CO_2 conditions (~400 µatm). (C,D) Embryos developing at control CO_2 conditions (~400 µatm), with one half of the replicates shifted pre-hatch to high CO_2 conditions (~2000 µatm). Thin dotted lines depict individual replicates; thick lines depict treatment means

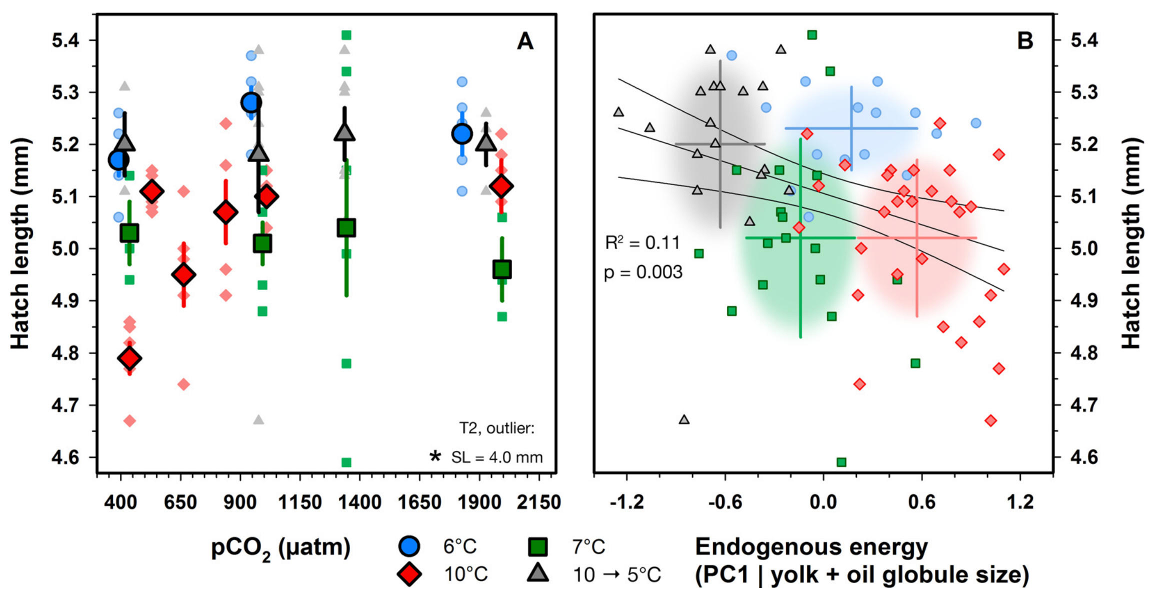

Fig. 4. Morphometrics of first *Ammodytes dubius* hatchlings (initial 4 d of hatch) in Expt 1 (6°C: blue circles; 10°C: red diamonds) and Expt 2 (7°C: green squares; 10→5°C: grey triangles). (A) CO_2-specific hatch standard length (SL), with small and large symbols depicting individual replicates and treatment means (±1 SE), respectively. (B) Relationship between hatch SL and endogenous energy reserves (PC1 of yolk sac size and oil globule size). Shading and bi-directional means (±SD) are given for each temperature treatment. Black lines: linear regression ±95% confidence intervals ($R^2 = 0.11$, $p = 0.003$)

significantly negatively related to hatch SL (linear regression, $R^2 = 0.11$, $p = 0.003$), i.e. larger hatchlings tended to have lower EER as approximated by their yolk and oil globule sizes (Fig. 4B). During Expt 2, mean hatch SL across all replicates increased over the course of the hatching period (linear regression, $R = 0.23$, $p = 0.008$), while EER declined steeply ($R = -0.50$, $p < 0.001$); hence, later hatched fish were only slightly larger but had severely reduced EERs compared to earlier hatchlings (Fig. 5).

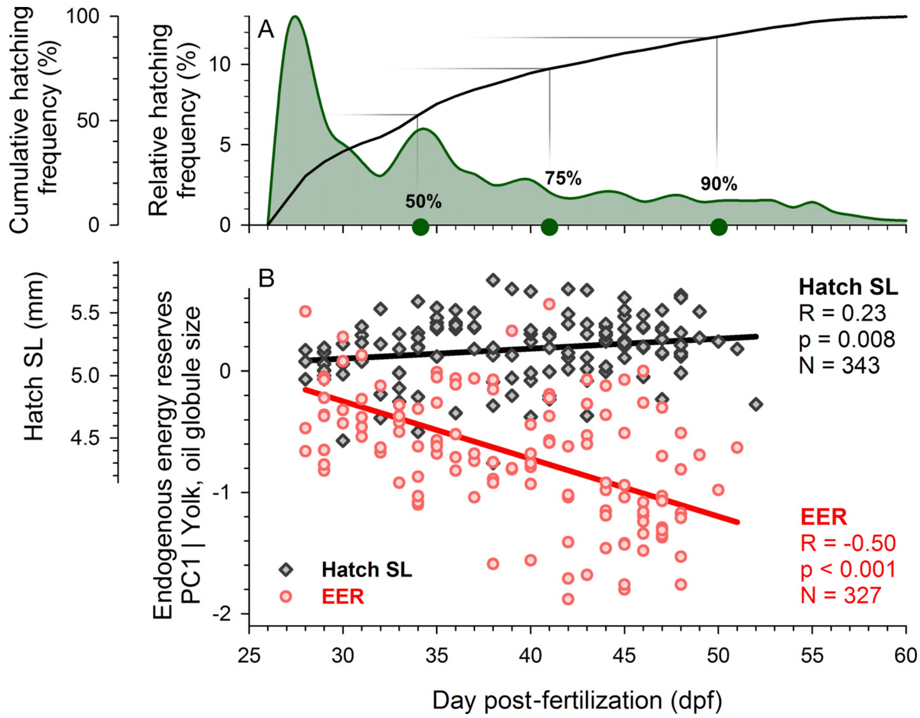

Fig. 5. (A) Overall relative (green shading) and cumulative (black line) *Ammodytes dubius* hatching frequencies in Expt 2, with 50%, 75%, and 90% hatched on 34, 41, and 50 dpf, respectively (green circles). (B) Changes in *A. dubius* hatch standard length (SL; grey diamonds, black line) and endogenous energy reserves (EER; red circles, red line) over the course of the hatching period during Expt 2. Each symbol represents a replicate mean regardless of temperature or pCO_2 treatment (outlier hatchlings: 7°C; 1700 µatm: not shown)

As expected, hatching phenology was strongly temperature-dependent during Expt 1 (GLM, $p \leq 0.001$; Table 2), because first and peak hatch occurred approximately 2 wk earlier at 10°C (19 and 21 dpf, respectively) than at 6°C (34 and 36 dpf, respectively), with the latter also having a significantly longer hatch period (6°C = 22 d, 10°C = 14 d; Fig. 6A). High pCO_2 slightly delayed the day of first hatch ($p = 0.001$) by approximately 1 d regardless of temperature (Fig. 6B). During Expt 2, static versus dynamic temperatures had no effect on first hatch (27 ± 0 dpf), peak hatch (33 ± 6.9 dpf) or hatching period (33 ± 1 d, GLM; Table 2), but increasing pCO_2 conditions significantly delayed peak hatch regardless of thermal conditions ($p < 0.001$; Fig. 6C).

Measurements of embryonic chorion thickness at 170 ddpf showed a significant positive pCO_2 effect regardless of temperature (Expt 1: GLM, pCO_2: $p = 0.035$, temperature: $p = 0.54$, no interaction), thus suggesting that embryos developing at high pCO_2 conditions had to hatch out of thicker chorions than their conspecifics at control pCO_2 levels (Fig. 7).

Regional simulations using RCP 8.5 (Siedlecki et al. 2021) predicted average seasonal pCO_2 fluctuations on Stellwagen Bank in 2050 between 526 µatm in October and 614 µatm in March (0–40 m, Fig. 8A). The range was provided by the 3 models used to project future conditions and reflects intra-model differences, as well as natural variability in the system. By 2100, pCO_2 concentrations were projected to double and seasonal fluctuations to triple, reaching 1084–1365 µatm (September, March; Fig. 8C). Mean winter projections (December–January) were 572 µatm (2050) and 1255 µatm pCO_2 (2100). After controlling for the different experiment- and temperature-specific baseline levels of HS in our study (HS_N, by normalizing to 100% HS at ~400 µatm pCO_2), the fitted linear relationship HS_N (%) = 116 − 0.036 × pCO_2 ($R^2 = 0.77$, $p < 0.001$, N = 17; Fig. 8B) implied a 7% decrease in HS for every 200 µatm increase in pCO_2. Hence, by the year 2100, sand lance HS would be reduced to 71% relative to contemporary HS levels (Fig. 8C).

4. DISCUSSION

Our study re-evaluated early-life CO_2 sensitivities in northern sand lance, a key forage fish and non-model species potentially vulnerable to future high CO_2 oceans. In both new experiments, we again observed large CO_2-induced reductions in hatching success (−23% and −61% at 1000 and 2000 µatm pCO_2, respectively), which are consistent with the main conclusion in Murray et al. (2019) that sand lance embryos are highly sensitive to CO_2. This has now been demonstrated by 4 independent trials in as many years (2016–2017: Murray et al. 2019; 2018–2020: present study), conducted by different primary experimenters (albeit in the same facility) on off-

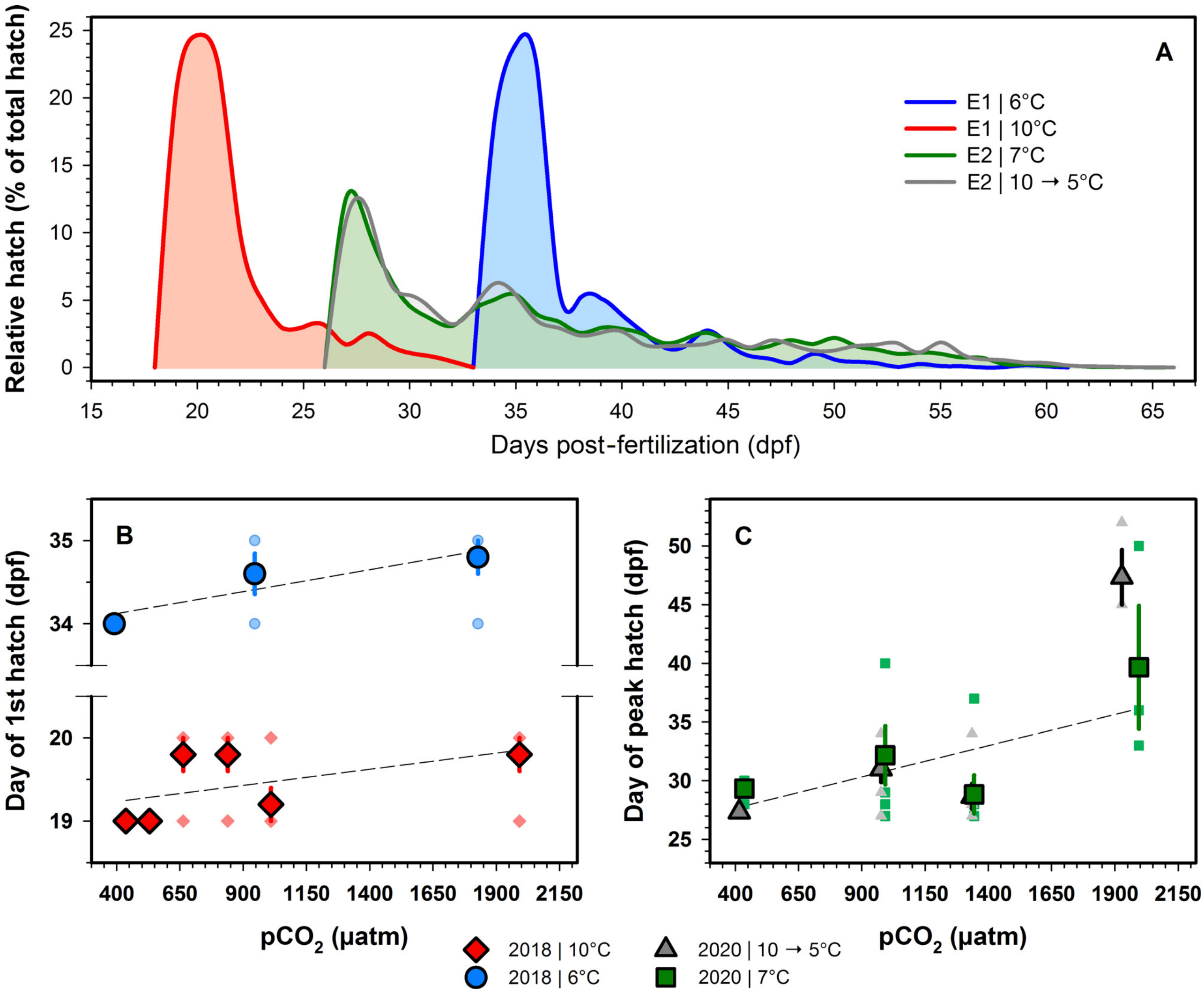

Fig. 6. *Ammodytes dubius* hatching dynamics in Expt 1 (E1; 6°C, 10°C) and Expt 2 (E2; 7°C, 10→5°C). (A) Experiment- and temperature-specific relative hatch frequencies according to day post-fertilization (dpf). (B) Expt 1: temperature- and pCO_2-specific day of first hatch. (C) Expt 2: temperature- and pCO_2-specific day of peak hatch. Small symbols: individual replicates; large symbols: mean

spring produced from wild, genetically diverse spawners. Thereby, the added empirical heterogeneity reduces the likelihood of spurious attribution to CO_2, which is the purpose of serial experimentation (Baumann et al. 2018). Conversely, while the initial data had suggested an increase in sand lance CO_2 sensitivity with temperature (10°C; Murray et al. 2019), CO_2-dependent hatching success in the present study was surprisingly similar at 6°C versus 10°C (Expt 1) or at static 7°C versus dynamic 10→5°C treatments (Expt 2). The reason for the different outcomes is unknown; however, the present study used twice as many CO_2 treatments at 10°C, higher levels of replication, and improved rearing protocols, which make the present findings more robust. In addition, a more eurythermic response is more realistic, because sand lance embryos must be adapted to the large seasonal temperature decline that they experience in their natural habitat (Suca et al. 2021). Indeed, during each year of experimentation, sand lance spawning on Stellwagen Bank occurred at approximately 10°C (H. Baumann pers. obs.), which is therefore unlikely to be a stressful temperature for the embryonic development of this species.

4.1. How exceptional is the CO_2 sensitivity of sand lance?

Our ability to compare sand lance to other high latitude fishes is unfortunately limited by the scarcity of tested species and differences between studies re-

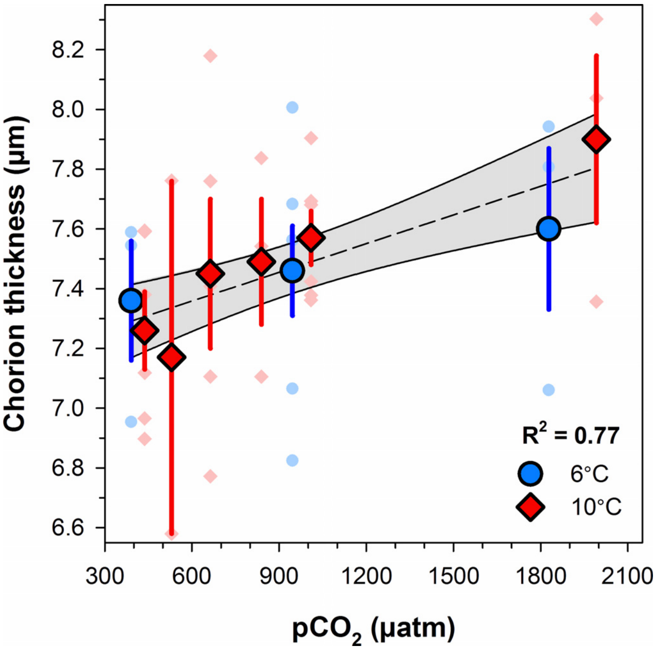

Fig. 7. CO_2-specific means (±1 SE) of chorion thickness around pre-hatch *Ammodytes dubius* embryos (Expt 1: 6°C: blue circles; 10°C: red diamonds) subsampled at 170 ddpf. Black lines depict linear regression ±95% confidence intervals (shading)

garding focal life stages, endpoints, pCO_2 levels, or sources of experimental fish. The clearest parallels exist for Barents Sea cod *Gadus morhua*, given the reported reductions in embryo survival of 11–47% in response to ~1100 µatm pCO_2 (Dahlke et al. 2017) and apparently similar post-hatch CO_2 sensitivities as demonstrated by Stiasny et al. (2016; showing a doubling of larval mortality rates in response to ~1200 µatm pCO_2). In Antarctic dragonfish *Gymnodraco acuticeps* embryos, survival was found to be sensitive to ~1000 µatm pCO_2 and warming, but the trials ended prior to hatch (Flynn et al. 2015). Conversely, experiments on summer flounder *Paralichthys dentatus* (offshore spawner) suggested large reductions in hatching success (−50%) at ~1800 relative to ~750 µatm pCO_2; however, this was based on offspring from just 3 females (Chambers et al. 2014). Poor genetic diversity or drift from wild populations may also underlie first reports of lethal CO_2 sensitivity in inland silverside *Menidia beryllina* embryos (−50% at ~1000 µatm; Baumann et al. 2012), which were sourced from a closed, commercial brood stock. We know today that co-occurring, congeneric Atlantic silversides *M. menidia*, when produced from wild spawners, are far more CO_2-tolerant (Baumann et al. 2018). Overall, however, fish early-life survival appears mostly robust to high pCO_2, as recently suggested by a meta-analysis (Cattano et al. 2018) that revealed no significant pCO_2 effects on embryo mortality (>1300 µatm) across all available species and contrasts (n = 13). Hence, the collective empirical evidence suggests that sand lance embryos are indeed unusual among fishes for their high CO_2 sensitivity, but whether this extends beyond the embryo stage has yet to be determined.

4.2. Why are sand lance embryos so CO_2 sensitive?

When CO_2-induced survival reductions occur in fish early life stages, the assumed cause of death is acidosis, a shorthand for the likely failure of pH-sensitive metabolic enzymes leading to arrested development due to ineffective acid–base regulation (Kikkawa et al. 2004, Esbaugh 2018). Yet most fishes appear to develop acid–base competency surprisingly early in life. For example, Dahlke et al. (2017, 2020) found that cod embryos remained CO_2-vulnerable only through the cleavage and gastrula stages (<50 ddpf), after which their ionocytes were sufficiently functional to tolerate CO_2 levels of 1100 µatm. Given that sand lance are likely adapted to offshore, low-CO_2 environments, their acid–base competency might develop more slowly, which therefore could have caused some of the CO_2-induced mortality that we observed in our experiments.

However, acidosis is unlikely to explain our observation that approximately one-fifth of sand lance embryos proceeded at high CO_2 conditions to fully pigmented, seemingly ready-to-hatch stages only to emerge delayed or not at all. This suggested that hatching itself was affected, perhaps because high CO_2 conditions reduced the efficiency of pH-sensitive hatching enzymes. Such proteolytic enzymes (chorionases) are ubiquitous in fish, produced by unicellular hatching glands and released into the perivitelline fluid to weaken the chorion before it can rupture and release the hatchling (Korwin-Kossakowski 2012). In most studied fishes, choreolytic enzymes work best at weakly alkaline conditions (e.g. Luberda et al. 1993, but see Shi et al. 2006), which implies that CO_2-induced acidification of the perivitelline fluid could impair enzyme activity and thus delay or impede hatching.

Our study provided 4 additional observations in support of the CO_2-impaired hatching hypothesis. First, when embryos were switched from high to control CO_2 conditions at 175 ddpf, their hatching success 2 d later improved in both 7°C and 10→5°C treatments, eventually reaching intermediate levels compared to unchanged embryos. This means that

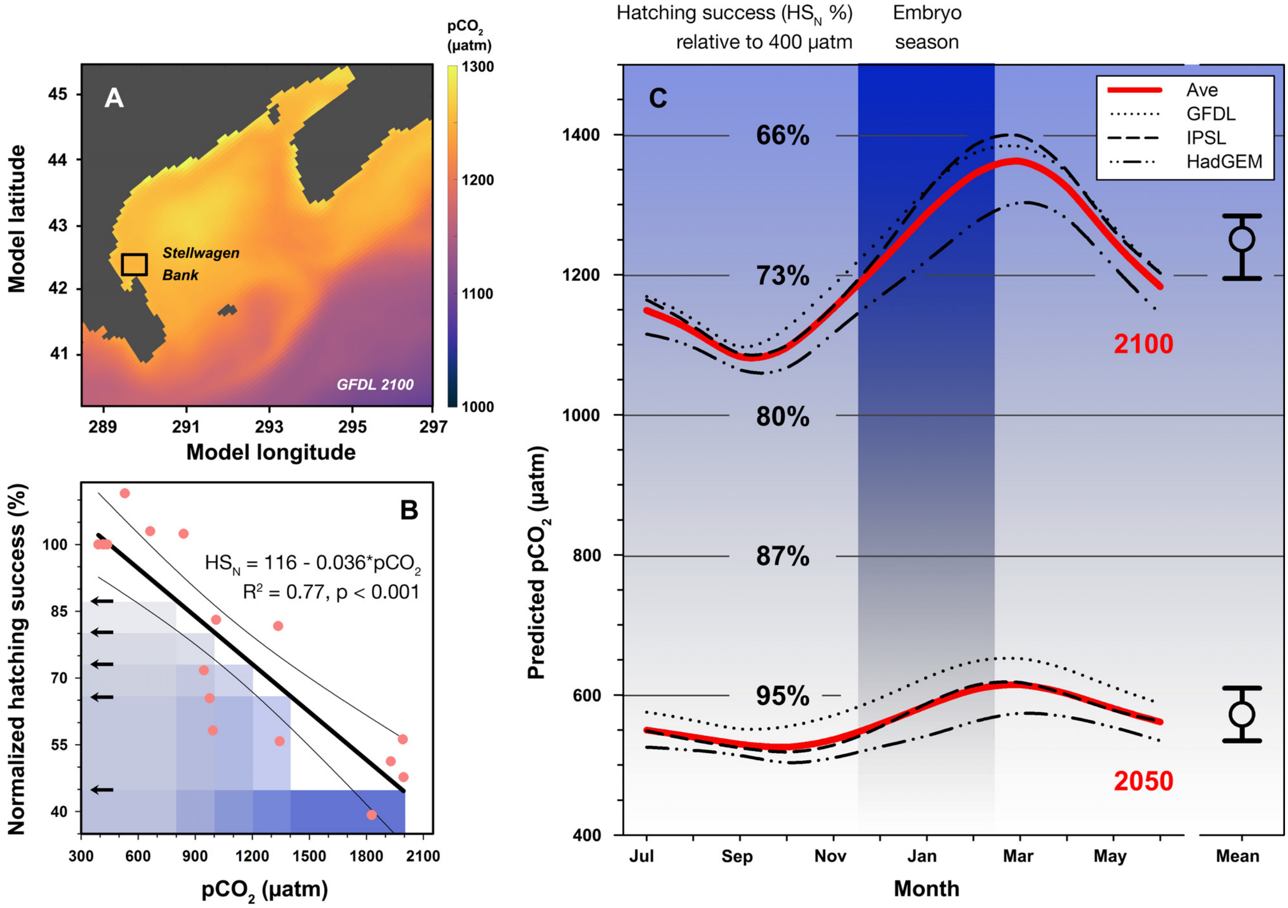

Fig. 8. CO_2-dependent sand lance hatching success (HS) in the context of regional pCO_2 projections. (A) Model domain including Gulf of Maine and adjacent Northwest-Atlantic shelf, subsampled for Stellwagen Bank (square; colors exemplify the GFDL pCO_2 forecast for November–January 2100). (B) Sand lance hatching success (Expts 1 and 2 combined) normalized to 400 µatm pCO_2 (HS_N) and used via linear regression to infer future pCO_2-induced reductions in HS_N. (C) Seasonal pCO_2 predictions for Stellwagen Bank (0–40 m) in years 2050 and 2100, based on 3 different models (black dotted and dashed lines, average = red line). Shading and isolines refer to the normalized hatching success of sand lance (HS_N). 'Mean' denotes projected average pCO_2 during the mean embryo season of sand lance (15 November–15 February, dark shaded area)

many embryos held at high CO_2 may have still been able to hatch at that point. The reverse was true, too, because the switch from control to high CO_2 immediately worsened hatching success, at least for the 7°C treatment. Given the larger hatch size in the 10→5°C treatments, it is possible that these more developed embryos had already initiated the hatching process at the time of the switch; too late for their hatching to suffer from the pCO_2 change. Second, high CO_2 conditions appeared to coincide with increased chorionic thickness (Expt 1, 170 ddpf), which presumably makes it harder for embryos to digest and rupture the chorion. However, more high-quality histological sections of individual embryos are needed to corroborate this finding in the future. Third, high CO_2 slightly delayed the day of first hatch in Expt 1, but led to significantly protracted hatching in Expt 2 (later peak hatch), which is consistent with observations by Murray et al. (2019). Delayed hatching implies that high CO_2 embryos struggled longer to rupture their chorion and hatch than their control CO_2 conspecifics. Fourth, sand lance embryos that hatched later during Expt 2 were of similar length but had progressively smaller endogenous energy reserves (i.e. the size of the yolk sac and oil globule). Hence, sand lance embryos struggling to hatch continued to expend energy without benefitting in terms of somatic growth. In nature, fish larvae with smaller yolk reserves have less time to successfully transition to external feeding (Houde 1997). Therefore, even if sand lance embryos eventually manage to hatch under high CO_2 conditions, they would suffer higher post-hatch mortalities from starvation or predation (Anderson 1988, Bailey & Houde 1989).

4.3. How soon could sand lance hatching be impacted in the wild?

Most experiments evaluating species CO_2 sensitivities employ common pCO_2 benchmarks derived from global models of average surface ocean acidification (Caldeira & Wickett 2003, Riebesell et al. 2011). To move beyond general implications, regional differences in future acidification trajectories can be considered when available (Bopp et al. 2013, Vargas et al. 2017). In the Gulf of Maine, for example, past decades of acidification appear to have been masked by stronger inflows of warm, high-salinity slope water (Salisbury & Jönsson 2018), with recent ensemble simulations diverging on how this process will continue (Siedlecki et al. 2021). Regardless, the seasonally explicit pCO_2 projections for Stellwagen Bank added valuable context to our experimental work. First, they suggest that sand lance hatching success should be robust to mid-century levels of predicted pCO_2 (500–650 µatm in 2050). Second, they reveal that seasonal pCO_2 fluctuations, which resemble northern hemisphere productivity cycles and thus attain their minima/maxima at the end of summer/winter, are likely to triple within this century (seasonal $\Delta pCO_{2;2050}$ = 88 µatm; $\Delta pCO_{2;2100}$ = 281 µatm), consistent with other modeling work (McNeil & Sasse 2016). The seasonality also entails that sand lance embryos actually experience slightly higher than annual average pCO_2 conditions, because they develop during winter months (December–February). Third, the predicted rise in winter pCO_2 to >1250 µatm by 2100 is more concerning, because according to our empirical data it could reduce sand lance hatching success by more than one-quarter (to 71 %). This reflects the linear, best fit to our overall data; however, a non-linear threshold response is also plausible, given that hatching success during Expt 1 remained around control levels until ~900 µatm pCO_2, before declining sharply. Unfortunately, this was only tested at one temperature (10°C, Expt 1) and therefore needs further corroboration.

4.4. What other factors may impact sand lance embryos?

At first glance, the projected reductions in sand lance hatching success may appear small, but it is worth recalling that much smaller relative changes in early-life survival are known to cause order-of-magnitude fluctuations in many marine fish populations (Sissenwine 1984). Moreover, many additional factors will ultimately modulate the climate vulnerability of sand lance, exerting direct and indirect, potentially positive and negative pressures on these important forage fish. For example, Suca et al. (2021) suggested that further warming in the Gulf of Maine could directly reduce sand lance overwinter survival and negatively affect recruitment via potential declines in the cold-water, lipid-rich copepod *Calanus finmarchicus* (Ji et al. 2017). Warming will also have multiple, potentially antagonistic effects on spawning phenology, as suggested by field observations and our experimental data. On the one hand, warmer autumn temperatures may delay the onset of spawning, because adults on Stellwagen Bank appear to use a ~10°C threshold as a cue (H. Baumann pers. obs.). On the other hand, embryo development and therefore hatching will accelerate at warmer conditions, as quantified in Expt 1 of this study, where first and peak hatch occurred 15 d earlier at 10°C compared to 6°C treatments (–3.75 d °C^{-1} warming). This is consistent with a 16 d earlier first and peak hatch at 10°C versus 5°C (–3.2 d °C^{-1} warming) measured by Murray et al. (2019) and pioneering experimental work by Smigielski et al. (1984) on American sand lance *A. americanus* (–4.3 d °C^{-1} warming). Depending on the net effect on hatching phenology, this could result in mismatches between emerging larvae and the first plankton bloom of the year (Dam & Baumann 2017). Furthermore, there was some empirical evidence (Fig. 2) that warming may reduce larval size at hatch, which implies lower first-feeding success and thus higher post-hatch mortalities in the future (Pepin 1991). Survival may also be sensitive to warming-related reductions in oxygen conditions (Keeling et al. 2010, Breitburg et al. 2018), but this has yet to be quantified experimentally for this species. Similarly, top-down effects could be altered by sand lance predators suffering unrelated declines and, therefore, relaxing predation pressure. Lastly, the relatively short generation time of sand lance (1–2 yr) may allow for evolutionary responses to warmer, high CO_2 oceans, but how fast fish and other metazoans may adapt to marine climate change is not yet well understood (Munday et al. 2019, Dam et al. 2021).

4.5. What are the critical knowledge gaps?

We argue that the discovery of CO_2-sensitive embryo survival in sand lance has far-reaching ecological and scientific implications and thus warrants further in-depth research on several fronts. First, we need empirical data on post-hatch CO_2 × temperature sensitivities in this species, which requires adjusted rearing methods and larger starting numbers of offspring. Second, it is imperative that we begin assessing other sand lance populations across the species' large geographic distribution, as well as congeners from Northeast Pacific and Northeast Atlantic ecosystems. For example, the congeneric American sand lance *A. americanus*, which occurs in nearshore US Atlantic habitats (Smigielski et al. 1984), might provide an important scientific contrast to the more offshore *A. dubius* — given the general decline in CO_2 variability from nearshore to offshore habitats and the expectation of concomitant declines in CO_2 tolerance (Vargas et al. 2017, Baumann 2019; ocean variability hypothesis). Third, targeted physiological assays should aim to better understand CO_2-impaired hatching in sand lance, specifically the question of whether CO_2 affects the amount made or the activity of the hatching enzyme, or may have other unrelated mechanisms. Given the ubiquity of pH-sensitive hatching enzymes in fishes, their potential CO_2-related impairment also deserves a broader look in other taxa. Finally, targeted crosses or genomic analyses could begin to resolve the evolutionary potential (=heredity) of CO_2-sensitive traits in sand lance (Johnson et al. 2010, Malvezzi et al. 2015), which would answer the question of whether evolutionary rescue is a possibility for fish species with highly CO_2-sensitive embryo stages.

Data availability. Citable source data are available from the BCO-DMO database [DOIs: 10.26008/1912/bco-dmo.867401.1; 10.26008/1912/bco-dmo.867447.1; 10.26008/1912/bco-dmo.867707.1; 10.26008/1912/bco-dmo.867837.1; 10.26008/1912/bco-dmo.867931.1]. Output from the three ROMS physical simulations used for the projections as well as the control run is provided on a website (www.psl.noaa.gov/ipcc/roms/) and described further in Alexander et al. (2020).

Acknowledgements. We thank C. Woods, J. Hamilton, M. Zavell, and J. Jones for their invaluable help in the lab, K. McGarry and J. Scott for their assistance with model data extractions, and the crew of the RV 'Auk' and D. Wiley, T. Silva, M. Thompson, and P. Hong for assistance in the field. We are grateful to the editor and 3 anonymous reviewers for their thoughtful comments on an earlier version of this manuscript. This work was partially funded by a Northeast Regional Sea Grant Consortium grant to H.B. (RNE16-CTHCE-l). Additional funding was provided by the Bureau of Ocean Energy Management IA agreement M17PG0019. S.A.S. acknowledges support from the NOAA Ocean Acidification Program (OAP) grant NA19OAR0170351.

LITERATURE CITED

Alexander MA, Shin Si, Scott JD, Curchitser E, Stock C (2020) The response of the Northwest Atlantic Ocean to climate change. J Clim 33:405–428

Alter K, Peck MA (2021) Ocean acidification but not elevated spring warming threatens a European seas predator. Sci Total Environ 782:146926

Anderson JT (1988) A review of size dependent survival during pre-recruit stages of fishes in relation to recruitment. J Northwest Atl Fish Sci 8:55–66

Ashur MM, Johnston NK, Dixson DL (2017) Impacts of ocean acidification on sensory function in marine organisms. Integr Comp Biol 57:63–80

Bailey KM, Houde ED (1989) Predation on eggs and larvae of marine fishes and the recruitment problem. Adv Mar Biol 25:1–83

Baumann H (2019) Experimental assessments of marine species sensitivities to ocean acidification and co-stressors: how far have we come? Can J Zool 97:399–408

Baumann H, Talmage SC, Gobler CJ (2012) Reduced early life growth and survival in a fish in direct response to increased carbon dioxide. Nat Clim Chang 2:38–41

Baumann H, Wallace R, Tagliaferri T, Gobler CJ (2015) Large natural pH, CO_2 and O_2 fluctuations in a temperate tidal salt marsh on diel, seasonal and interannual time scales. Estuaries Coasts 38:220–231

Baumann H, Cross EL, Murray CS (2018) Robust quantification of fish early life CO_2 sensitivities via serial experimentation. Biol Lett 14:20180408

Bignami S, Enochs IC, Manzello DP, Sponaugle S, Cowen RK (2013) Ocean acidification alters the otoliths of a pantropical fish species with implications for sensory function. Proc Natl Acad Sci USA 110:7366–7370

Bopp L, Resplandy L, Orr JC, Doney SC and others (2013) Multiple stressors of ocean ecosystems in the 21st century: projections with CMIP5 models. Biogeosciences 10: 6225–6245

Boyd PW, Collins S, Dupont S, Fabricius K and others (2018) Experimental strategies to assess the biological ramifications of multiple drivers of global ocean change — A review. Glob Change Biol 24:2239–2261

Breitburg D, Levin LA, Oschlies A, Grégoire M and others (2018) Declining oxygen in the global ocean and coastal waters. Science 359:eaam7240

Brickman D, Alexander MA, Pershing A, Scott JD, Wang Z (2021) Projections of physical conditions in the Gulf of Maine in 2050. Elem Sci Anth 9:00055

Busch DS, O'Donnell MJ, Hauri C, Mach KJ, Poach M, Doney SC, Signorini SR (2015) Understanding, characterizing, and communicating responses to ocean acidification: challenges and uncertainties. Oceanography 28:30–39

Caldeira K, Wickett ME (2003) Anthropogenic carbon and ocean pH. Nature 425:365

Cattano C, Claudet J, Domenici P, Milazzo M (2018) Living in a high CO_2 world: a global meta-analysis shows multiple trait-mediated fish responses to ocean acidification. Ecol Monogr 88:320–335

Chambers RC, Candelmo AC, Habeck EA, Poach ME and others (2014) Effects of elevated CO_2 in the early life stages of summer flounder, *Paralichthys dentatus*, and potential consequences of ocean acidification. Biogeosciences 11:1613–1626

Concannon CA, Cross EL, Jones LF, Murray CS, Matassa C, McBride RS, Baumann H (2021) Whole-life, high-CO_2 exposure affects temperature-dependent fecundity traits in a serial broadcast spawning fish. ICES J Mar Sci 78: 3724–3734

Crespel A, Anttila K, Lelièvre P, Quazuguel P and others (2019) Long-term effects of ocean acidification upon

energetics and oxygen transport in the European sea bass (*Dicentrarchus labrax*, Linnaeus). Mar Biol 166:1–12
Dahlke FT, Leo E, Mark FC, Pörtner HO, Bickmeyer U, Frickenhaus S, Storch D (2017) Effects of ocean acidification increase embryonic sensitivity to thermal extremes in Atlantic cod, *Gadus morhua*. Glob Change Biol 23: 1499–1510
Dahlke F, Lucassen M, Bickmeyer U, Wohlrab S and others (2020) Fish embryo vulnerability to combined acidification and warming coincides with a low capacity for homeostatic regulation. J Exp Biol 223:jeb212589
Dam HG, Baumann H (2017) Climate change, zooplankton and fisheries. In: Phillips B, Pérez-Ramírez M (eds) The impacts of climate change on fisheries and aquaculture. Wiley/Blackwell, Hoboken, NJ
Dam HG, deMayo JA, Park G, Norton L and others (2021) Rapid, but limited, zooplankton adaptation to simultaneous warming and acidification. Nat Clim Chang 11:780–786
Depasquale E, Baumann H, Gobler CJ (2015) Variation in early life stage vulnerability among Northwest Atlantic estuarine forage fish to ocean acidification and low oxygen. Mar Ecol Prog Ser 523:145–156
Donelson JM, Salinas S, Munday PL, Shama LN (2018) Transgenerational plasticity and climate change experiments: Where do we go from here? Glob Change Biol 24: 13–34
Doney SC, Busch DS, Cooley SR, Kroeker KJ (2020) The impacts of ocean acidification on marine ecosystems and reliant human communities. Annu Rev Environ Resour 45:83–112
Esbaugh AJ (2018) Physiological implications of ocean acidification for marine fish: emerging patterns and new insights. J Comp Physiol B 188:1–13
Faria AM, Lopes AF, Silva CSE, Novais SC, Lemos MFL, Gonçalves EJ (2018) Reproductive trade-offs in a temperate reef fish under high *p*CO2 levels. Mar Environ Res 137:8–15
Flynn EE, Bjelde BE, Miller NA, Todgham AE (2015) Ocean acidification exerts negative effects during warming conditions in a developing Antarctic fish. Conserv Physiol 3:cov033
Franke A, Clemmesen C (2011) Effect of ocean acidification on early life stages of Atlantic herring (*Clupea harengus* L.). Biogeosciences 8:3697–3707
Garcia-Soto C, Cheng L, Caesar L, Schmidtko S and others (2021) An overview of ocean climate change indicators: sea surface temperature, ocean heat content, ocean pH, dissolved oxygen concentration, Arctic sea ice extent, thickness and volume, sea level and strength of the AMOC (Atlantic Meridional Overturning Circulation). Front Mar Sci 8:642372
Harvey BP, Gwynn-Jones D, Moore PJ (2013) Meta-analysis reveals complex marine biological responses to the interactive effects of ocean acidification and warming. Ecol Evol 3:1016–1030
Heuer RM, Grosell M (2014) Physiological impacts of elevated carbon dioxide and ocean acidification on fish. Am J Physiol Regul Integr Comp Physiol 307:R1061–R1084
Hofmann GE, Smith JE, Johnson KS, Send U and others (2011) High-frequency dynamics of ocean pH: A multi-ecosystem comparison. PLOS ONE 6:e28983
Houde ED (1997) Patterns and consequences of selective processes in teleost early life histories. Early life history and recruitment in fish populations. Springer, Dordrecht, p 173–196
Ji R, Feng Z, Jones BT, Thompson C, Chen C, Record NR, Runge JA (2017) Coastal amplification of supply and transport (CAST): a new hypothesis about the persistence of *Calanus finmarchicus* in the Gulf of Maine. ICES J Mar Sci 74:1865–1874
Johnson DW, Christie MR, Moye J (2010) Quantifying evolutionary potential of marine fish larvae: heritability, selection, and evolutionary constraints. Evolution 64: 2614–2628
Keeling RF, Körtzinger A, Gruber N (2010) Ocean deoxygenation in a warming world. Annu Rev Mar Sci 2:199–229
Kelly MW, Padilla-Gamiño JL, Hofmann GE (2013) Natural variation and the capacity to adapt to ocean acidification in the keystone sea urchin *Strongylocentrotus purpuratus*. Glob Change Biol 19:2536–2546
Kikkawa T, Kita J, Ishimatsu A (2004) Comparison of the lethal effect of CO_2 and acidification on red sea bream (*Pagrus major*) during the early developmental stages. Mar Pollut Bull 48:108–110
Korwin-Kossakowski M (2012) Fish hatching strategies: a review. Rev Fish Biol Fish 22:225–240
Kroeker KJ, Kordas RL, Crim RN, Singh GG (2010) Meta-analysis reveals negative yet variable effects of ocean acidification on marine organisms. Ecol Lett 13: 1419–1434
Kroeker KJ, Kordas RL, Crim R, Hendriks IE and others (2013) Impacts of ocean acidification on marine organisms: quantifying sensitivities and interaction with warming. Glob Change Biol 19:1884–1896
Lonthair J, Ern R, Esbaugh AJ (2017) The early life stages of an estuarine fish, the red drum (*Sciaenops ocellatus*), are tolerant to high pCO_2. ICES J Mar Sci 74:1042–1050
Lotterhos KE, Láruson ÁJ, Jiang LQ (2021) Novel and disappearing climates in the global surface ocean from 1800 to 2100. Sci Rep 11: 15535
Luberda Z, Strzezek J, Luczynski M (1993) Some proteolytic properties of hatching liquid in the sea trout, *Salmo trutta m. trutta* L. Fish Physiol Biochem 12:75–80
Malvezzi AJ, Murray CS, Feldheim KA, Dibattista JD and others (2015) A quantitative genetic approach to assess the evolutionary potential of a coastal marine fish to ocean acidification. Evol Appl 8:352–362
Mazurais D, Servili A, Noel C, Cormier A and others (2020) Transgenerational regulation of cbln11 gene expression in the olfactory rosette of the European sea bass (*Dicentrarchus labrax*) exposed to ocean acidification. Mar Environ Res 159:105022
McGarry K, Siedlecki SR, Salisbury J, Alin SA (2021) Multiple linear regression models for reconstructing and exploring processes controlling the carbonate system of the northeast US from basic hydrographic data. J Geophys Res Oceans 126:e2020JC016480
McNeil BI, Sasse TP (2016) Future ocean hypercapnia driven by anthropogenic amplification of the natural CO_2 cycle. Nature 529:383–386
Munday PL, Crawley NE, Nilsson GE (2009) Interacting effects of elevated temperature and ocean acidification on the aerobic performance of coral reef fishes. Mar Ecol Prog Ser 388:235–242
Munday PL, McCormick MI, Meekan M, Dixson DL, Watson SA, Chivers DP, Ferrari MC (2012) Selective mortality associated with variation in CO_2 tolerance in a marine fish. Ocean Acidif 1:1–5
Munday PL, Watson SA, Parsons DM, King A and others (2016) Effects of elevated CO_2 on early life history devel-

opment of the yellowtail kingfish, *Seriola lalandi*, a large pelagic fish. ICES J Mar Sci 73:641–649

Munday PL, Rummer JL, Baumann H (2019) Adaptation and evolutionary responses to high CO_2. In: Grosell M, Munday PL, Brauner C, Farell AP (eds) Fish physiology, Vol 37: carbon dioxide. Academic Press, Cambridge, MA, p 369–395

Murray CS, Baumann H (2018) You better repeat it: complex temperature × CO_2 effects in Atlantic silverside offspring revealed by serial experimentation. Diversity 10:1–19

Murray CS, Baumann H (2020) Are long-term growth responses to elevated pCO_2 sex-specific in fish? PLOS ONE 15:e0235817

Murray CS, Malvezzi AJ, Gobler CJ, Baumann H (2014) Offspring sensitivity to ocean acidification changes seasonally in a coastal marine fish. Mar Ecol Prog Ser 504:1–11

Murray CS, Wiley D, Baumann H (2019) High sensitivity of a keystone forage fish to elevated CO_2 and temperature. Conserv Physiol 7: coz084

Pepin P (1991) Effect of temperature and size on development, mortality, and survival rates of the pelagic early life history stages of marine fish. Can J Fish Aquat Sci 48: 503–518

Perry DM, Redman DH, Widman JC, Meseck S, King A, Pereira JJ (2015) Effect of ocean acidification on growth and otolith condition of juvenile scup, *Stenotomus chrysops*. Ecol Evol 5:4187–4196

Pierrot D, Lewis E, Wallace D (2006) MS Excel program developed for CO_2 system calculations. ORNL/CDIAC-105a Carbon Dioxide Information Analysis Center, Oak Ridge National Laboratory, US Department of Energy, Oak Ridge, TN. https://cdiac.ess-dive.lbl.gov/ftp/co2sys/CO2SYS_calc_XLS_v2.1/

Pimentel M, Pegado M, Repolho T, Rosa R (2014) Impact of ocean acidification in the metabolism and swimming behavior of the dolphinfish (*Coryphaena hippurus*) early larvae. Mar Biol 161:725–729

Porteus CS, Hubbard PC, Webster TMU, van Aerle R, Canário AV, Santos EM, Wilson RW (2018) Near-future CO_2 levels impair the olfactory system of a marine fish. Nat Clim Chang 8:737–746

Przeslawski R, Byrne M, Mellin C (2015) A review and meta-analysis of the effects of multiple abiotic stressors on marine embryos and larvae. Glob Change Biol 21:2122–2140

Riebesell U, Fabry VJ, Hansson L, Gattuso JP (2011) Guide to best practices for ocean acidification research and data reporting. Publications Office of the European Union, Luxembourg

Robards MD, Willson MF, Armstrong RH, Piatt JF (2000) Sand lance: a review of biology and predator relations and annotated bibliography. PNW-RP-521. USDA, Portland, OR

Salisbury JE, Jönsson BF (2018) Rapid warming and salinity changes in the Gulf of Maine alter surface ocean carbonate parameters and hide ocean acidification. Biogeochemistry 141:401–418

Shi ZP, Fan TJ, Cong RS, Wang XF, Sun WJ, Yang LL (2006) Purification and characterization of hatching enzyme from flounder *Paralichthys olivaceus*. Fish Physiol Biochem 32:35–42

Siedlecki S, Salisbury J, Gledhill D, Bastidas C and others (2021) Projecting ocean acidification impacts for the Gulf of Maine to 2050: new tools and expectations. Elem Sci Anth 9:00062

Silva TL, Wiley DN, Thompson MA, Hong P and others (2020) High collocation of sand lance and protected top predators: implications for conservation and management. Conserv Sci Pract 3:e274

Sissenwine MP (1984) Why do fish populations vary? In: May R (ed) Exploitation of marine communities. Springer-Verlag, Berlin, p 59–94

Smigielski AS, Halavik TA, Buckley LJ, Drew SM, Laurence GC (1984) Spawning, embryo development and growth of the American sand lance *Ammodytes americanus* in the laboratory. Mar Ecol Prog Ser 14:287–292

Staudinger MD, Goyert H, Suca JJ, Coleman K and others (2020) The role of sand lances (*Ammodytes* sp.) in the Northwest Atlantic Ecosystem: a synthesis of current knowledge with implications for conservation and management. Fish Fish 21:522–556

Stiasny MH, Mittermayer FH, Sswat M, Voss R and others (2016) Ocean acidification effects on Atlantic cod larval survival and recruitment to the fished population. PLOS ONE 11:e0155448

Suca JJ, Wiley DN, Silva TL, Robuck AR and others (2021) Sensitivity of sand lance to shifting prey and hydrography indicates forthcoming change to the northeast US shelf forage fish complex. ICES J Mar Sci 78: 1023–1037

Sunday JM, Calosi P, Dupont S, Munday PL, Stillman JH, Reusch TBH (2014) Evolution in an acidifying ocean. Trends Ecol Evol 29:117–125

Vargas CA, Lagos NA, Lardies MA, Duarte C and others (2017) Species-specific responses to ocean acidification should account for local adaptation and adaptive plasticity. Nat Ecol Evol 1:0084

Editorial responsibility: Alistair Hobday, Hobart, Tasmania, Australia
Reviewed by: 3 anonymous referees

Submitted: November 18, 2021
Accepted: February 1, 2022
Proofs received from author(s): April 3, 2022